Chapter 12

Numerical Simulation of Wave (Shock Profile) Propagation of the Kuramoto-Sivashinsky Equation Using an Adaptive Mesh Method

Denson Muzadziwa, Stephen T. Sikwila and Stanford Shateyi

Additional information is available at the end of the chapter

http://dx.doi.org/10.5772/intechopen.71875

Abstract

In this paper, the Kuramoto-Sivashinsky equation is solved using Hermite collocation method on an adaptive mesh. The method uses seventh order Hermite basis functions on a mesh that is adaptive in space. Numerical experiments are carried out to validate effectiveness of the method.

Keywords: adaptive mesh method, Kuramoto-Sivashinsky equation, collocation method, moving mesh partial differential equation, numerical solution

1. Introduction

The Kuramoto-Sivashinsky equation (KSe) is a non-linear fourth order partial differential equation (PDE) discovered separately by Kuramoto and Sivashinsky in the study of non-linear stability of travelling waves. Sivashinsky [1] came up with the equation while modelling small thermal diffusive instabilities in laminar flame fronts. Kuramoto [2–5] derived the equation in the study of the Belousov-Zhabotinsky reaction as a model of diffusion induced chaos. The KSe is of interest to many researchers because of its ability to describe several physical contexts such as long waves on thin films or on the interface between two viscous fluids [6] and unstable drift waves in plasmas. The equation is also used as a model to describe spatially uniform oscillating chemical reaction in a homogeneous medium and fluctuations in fluid films on inclines [7]. In one dimension, consider the KSe of the form

$$\frac{\partial u}{\partial t} + u\frac{\partial u}{\partial x} + \frac{\partial^2 u}{\partial x^2} + \frac{\partial^4 u}{\partial x^4} = 0, \qquad t > 0. \tag{1}$$

The second derivative term is an energy source and thus has a distributing effect. The non-linear term is a correction to the phase speed and responsible for transferring energy. The fourth derivative term is the dominating term and is responsible for stabilising the equation. Several methods have been used to solve the KSe numerically and these include Chebyshev spectral collocation method [8], Quintic B-spline collocation method [9], Lattice Boltzmann method [10], meshless method of lines [11], Fourier spectral method [12] and septic B-spline collocation method [13].

2. Grid generation

Generation of an adaptive mesh in the spatial domain is based on the r-refinement technique [14] which relocates a fixed number of nodal points to regions which need high spatial resolution in order to capture important characteristics in the solution. This has the benefit of improving computational effort in those regions of interest whilst using a fixed number of mesh points. The relocation of the fixed number of nodal points at any given time is achieved by solving Moving Mesh Partial Differential Equations (MMPDEs) [15, 16] derived from the Equidistribution Principle (EP). The EP [17] makes use of a measure of the solution error called a monitor function, denoted by M which is a positive definite and user defined function of the solution and/or its derivatives. Mesh points are then chosen by equally distributing the error in each subinterval. In this paper, MMPDE4 [15] is chosen to generate the adaptive mesh because of its ability to stabilise mesh trajectories and ability to give unique solutions for the mesh velocities with Dirichlet boundary conditions. MMPDE4 is given by

$$\frac{\partial}{\partial \xi}\left(M\frac{(\partial \dot{x})}{\partial \xi}\right) = -\frac{1}{\tau}\frac{\partial}{\partial \xi}\left(M\frac{\partial x}{\partial \xi}\right) \tag{2}$$

where τ is the relaxation parameter and it plays the role of driving the mesh towards equidistribution. Central finite difference approximation of MMPDE4 in space on the interval $a \le x \le b$ gives

$$\frac{M_{i+1}+M_i}{2\left(\frac{1}{N}\right)^2}(\dot{x}_{i+1}-\dot{x}_i) - \frac{M_i+M_{i-1}}{2\left(\frac{1}{N}\right)^2}(\dot{x}_i-\dot{x}_{i-1}) = -\frac{E_i}{\tau}, \tag{3}$$

where

$$E_i = \frac{M_{i+1}+M_i}{2\left(\frac{1}{N}\right)^2}(x_{i+1}-x_i) - \frac{M_i+M_{i-1}}{2\left(\frac{1}{N}\right)^2}(x_i-x_{i-1}), \qquad i = 2, \ldots, N \tag{4}$$

$$x_1 = a \qquad\qquad x_{N+1} = b. \tag{5}$$

The modified monitor function given by

$$M(x,t) = \left(1 + \alpha^2\left(\frac{\partial u}{\partial x}\right)^2 + \alpha^2\left(\frac{\partial^2 u}{\partial x^2}\right)^2\right)^{\frac{1}{2}} \tag{6}$$

is used. It is composed of the standard arc-length monitor and the curvature monitor functions. Smoothing on the monitor function is done as described in [15]. Values of the smoothed monitor function $\tilde{M}$ at the grid points are given by

$$\widetilde{M} = \sqrt{\frac{\sum_{k=i-p}^{i+p} (M_k)^2 \left(\frac{\gamma}{1+\gamma}\right)^{|k-i|}}{\sum_{k=i-p}^{i+p} \left(\frac{\gamma}{1-\gamma}\right)^{|k-i|}}} \tag{7}$$

where the parameter p is called the smoothing index which determines the extent of smoothing and is non-negative. γ is non-negative and is called the smoothing index and determines the rigidity of the grid.

3. Discretization in time

The Crank-Nicolson scheme for the KSe is

$$\left[\frac{u^{n+1} - u^n}{\delta t}\right] + \left[\frac{(uu_x)^{n+1} + (uu_x)^n}{2}\right] + \left[\frac{u_{xx}^{n+1} + u_{xx}^n}{2}\right] + \left[\frac{u_{xxxx}^{n+1} + u_{xxxx}^n}{2}\right] = 0 \tag{8}$$

where δt is the time step. Rubin and Graves [18] suggested the expression

$$uu_x{}^{n+1} = u^{n+1}u_x^n + u^n u_x^{n+1} - (uu_x)^n \tag{9}$$

for the linearization of the non-linear term $(uu_x)^{n+1}$. Expression (9) is substituted into (1) and the terms are rearranged to give

$$u^{n+1} + \frac{\delta t}{2}\left[u^{n+1}u_x^n + u^n u_x^{n+1} + u_{xx}^{n+1} + u_{xxxx}^{n+1}\right] = u^n - \frac{\delta t}{2}\left[u_{xx}^n + u_{xxxx}^n\right] \tag{10}$$

4. Septic Hermite collocation method

Consider the mesh on the domain $[a, b]$ which is a solution of MMPDE4 given by

$$a = X_1(t) < X_2(t) < \ldots < X_{N+1}(t) = b \tag{11}$$

The variable spatial length of each interval is given by H_i where $H_i = X_{i+1}(t) - X_i(t)$ for $i = 1, \ldots, N$. For some $x\epsilon[X_i(t), X_{i+1}(t)]$, define the local variable s as

$$s = \frac{x - X_i(t)}{H_i(t)} \tag{12}$$

such that $s\epsilon(0, 1)$ for every subinterval of the mesh (11). Define the septic Hermite basis functions with the local variables s as

$$
\begin{aligned}
L_{0,0} &= \left(20s^3 + 10s^2 + 4s + 1\right)(s-1)^4 \\
L_{0,1} &= s\left(10s^2 + 4s + 1\right)(s-1)^4 \\
L_{0,2} &= \frac{s^2}{2}(4s+1)(s-1)^4 \\
L_{0,3} &= \frac{s^3}{6}(s-1)^4 \\
L_{1,0} &= -\left(20s^3 - 70s^2 + 84s - 35\right)s^4 \\
L_{1,2} &= -\frac{s^4}{2}(s-1)^2(4s-5) \\
L_{1,3} &= \frac{s^4}{6}(s-1)^3
\end{aligned}
\tag{13}
$$

For $l = 0, 1, 2, 3$ the functions $L_{0,l}(s)$ and $L_{1,l}(s)$ yield the following conditions

$$
\begin{aligned}
&\frac{d^k}{ds^k}L_{0,l}(0) = \delta_{k,l}, \qquad \frac{d^k}{ds^k}L_{0,l}(1) = 0, \qquad k, l = 0, 1, 2, 3 \\
&\frac{d^k}{ds^k}L_{0,l}(0) = 0, \qquad \frac{d^k}{ds^k}L_{1,l}(1) = \delta_{k,l}, \qquad k, l = 0, 1, 2, 3
\end{aligned}
$$

where $\delta_{k,l}$ denotes the Kronecker delta. The physical solution $u(x,t)$ on the mesh (11) is approximated by the piecewise Hermite polynomial [19]

$$
\begin{aligned}
U(x,t) = {} & U_i(t)L_{0,0}(s) + U_{x,i}H_i(t)L_{0,1}(s) + U_{xx,i}(t)H_i^2(t)L_{0,2}(s) + U_{xxx,i}(t)H_i^3(t)L_{0,3}(s) \\
& + U_{i+1}(t)L_{1,0}(s) + U_{x,i+1}H_i(t)L_{1,1}(s) + U_{xx,i+1}(t)H_i^2(t)L_{1,2}(s) + U_{xxx,i+1}(t)H_i^3(t)L_{1,3}(s),
\end{aligned}
\tag{14}
$$

Where $U_i(t)$, $U_{x,i}(t)$, $U_{xx,i}(t)$ and $U_{xxx,i}(t)$ are the unknown variables. Derivatives of $U(x,t)$ with respect to the spatial variable x for $x \in [X_i(t), X_{i+1}(t)]$ are obtained by direct differentiation of (14) to give

$$
\begin{aligned}
\frac{\partial^{(l)}U(x,t)}{\partial x^{(l)}} = \frac{1}{H_i(t)^{(l)}} \Bigg[& U_i(t)\frac{d^{(l)}L_{0,0}}{ds^{(l)}} + U_{x,i}(t)H_i(t)\frac{d^{(l)}L_{0,1}}{ds^{(l)}} + U_{xx,i}(t)H_i^2(t)\frac{d^{(l)}L_{0,2}}{ds^{(l)}} \\
& + U_{xxx,i}(t)H_i^3(t)\frac{d^{(l)}L_{0,3}}{ds^{(l)}} + U_{i+1}(t)\frac{d^{(l)}L_{1,0}}{ds^{(l)}} + U_{x,i+1}(t)H_i(t)\frac{d^{(l)}L_{1,1}}{ds^{(l)}} \\
& + U_{xx,i+1}(t)H_i^2(t)\frac{d^{(l)}L_{1,2}}{ds^{(l)}} + U_{xxx,i+1}(t)H_i^3(t)\frac{d^{(l)}L_{1,3}}{ds^{(l)}} \Bigg]
\end{aligned}
\tag{15}
$$

for $l = 1, 2, 3, 4$. In each subinterval $[X_i(t), X_{i+1}(t)]$ of the mesh (11), define four Gauss-Legendre points

$$0 < \rho_1 < \rho_2 < \rho_3 < \rho_4 < 1$$

which are given by

$$\rho_1 = \frac{1}{2} - \frac{\sqrt{525 + 70\sqrt{30}}}{70}$$

$$\rho_2 = \frac{1}{2} - \frac{\sqrt{525 - 70\sqrt{30}}}{70}$$

$$\rho_3 = 1 - \rho_1$$

$$\rho_4 = 1 - \rho_2$$

One regards these points as the collocation points in each subinterval of the mesh (11). Scaling of the Gauss-Legendre points into subsequent intervals is done by defining the collocation points as

$$X_{ij} = X_i + H_i\rho_j, \quad i = 1, \ldots, N, \quad j = 1, 2, 3, 4. \tag{16}$$

and redefining the local variable s as

$$s_j^{(i)} = \frac{X_{ij} - X_i}{H_i} \tag{17}$$

for $i = 1, \ldots, N$ and $j = 1, 2, 3, 4$. Evaluation of the Hermite polynomial approximation (14), its first, second and fourth derivatives (15) is then done at the four internal collocation points in each subinterval $[X_i, X_{i+1}]$ and substitution of the expressions into (10) gives the difference equation

$$\beta_{j1}^{(i)}U_i^{n+1} + \beta_{j2}^{(i)}U_{x,i}^{n+1} + \beta_{j3}^{(i)}U_{xx,i}^{n+1} + \beta_{j4}^{(i)}U_{xxx,i}^{n+1} + \beta_{j5}^{(i)}U_{i+1}^{n+1} + \beta_{j6}^{(i)}U_{x,i+1}^{n+1} + \beta_{j7}^{(i)}U_{xx,i+1}^{n+1} + \beta_{j8}^{(i)}U_{xxx,i+1}^{n+1} = \psi_{ij}^n \tag{18}$$

where

$$\begin{aligned}
\psi_{ij}^n = {} & U_i^n(t)L_{0,0}(s_j) + U_{x,i}^n H_i(t)L_{0,1}(s_j) + U_{xx,i}^n(t)H_i^2(t)L_{0,2}(s_j) + U_{xxx,i}^n(t)H_i^3(t)L_{0,3}(s_j) \\
& + U_{i+1}^n(t)L_{1,0}(s_j) + U_{x,i+1}^n H_i(t)L_{1,1}(s_j) + U_{xx,i+1}^n H_i(t)L_{1,1}(s_j) + U_{xxx,i+1}^n H_i(t)L_{1,1}(s_j) \\
& - \frac{\delta t}{2H_i^2}\Big[U_i^n(t)L_{0,0}''(s_j) + U_{x,i}^n H_i(t)L_{0,1}''(s_j) + U_{xx,i}^n(t)H_i^2(t)L_{0,2}''(s_j) + U_{xxx,i}^n(t)H_i^3(t)L_{0,3}''(s_j) \\
& + U_{i+1}^n(t)L_{1,0}''(s_j) + U_{x,i+1}^n H_i(t)L_{1,1}''(s_j) + U_{xx,i+1}^n H_i(t)L_{1,1}''(s_j) + U_{xxx,i+1}^n H_i(t)L_{1,1}''(s_j)\Big] \\
& - \frac{\delta t}{2H_i^4}\Big[U_i^n(t)L_{0,0}^{(iv)}(s_j) + U_{x,i}^n H_i(t)L_{0,1}^{(iv)}(s_j) + U_{xx,i}^n(t)H_i^2(t)L_{0,2}^{(iv)}(s_j) + U_{xxx,i}^n(t)H_i^3(t)L_{0,3}^{iv}(s_j) \\
& + U_{i+1}^n(t)L_{1,0}^{(iv)}(s_j) + U_{x,i+1}^n H_i(t)L_{1,1}^{(iv)}(s_j) + U_{xx,i+1}^n H_i(t)L_{1,1}^{(iv)}(s_j) + U_{xxx,i+1}^n H_i(t)L_{1,1}^{(iv)}(s_j)\Big]
\end{aligned} \tag{19}$$

and

$$
\begin{aligned}
\beta_{j1}^{(i)} &= L_{0,0}(s_j) + \frac{\delta t}{2} U_{x,i}^n L_{0,0}(s_j) + \frac{\delta t}{2H_i(t)} U_i^n L'_{0,0}(s_j) + \frac{\delta t}{2H_i^2(t)} L''_{0,0}(s_j) + \frac{\delta t}{2H_i^2(t)} L_{0,0}^{(iv)}(s_j) \\
\beta_{j2}^{(i)} &= H_i(t) L_{0,1}(s_j) + \frac{\delta t}{2} U_{x,i}^n H_i(t) L_{0,1}(s_j) + \frac{\delta t}{2H_i(t)} U_i^n H_i(t) L'_{0,1}(s_j) + \frac{\delta t}{2H_i^2(t)} H_i(t) L''_{0,1}(s_j) + \frac{\delta t}{2H_i^2(t)} H_i(t) L_{0,1}^{(iv)}(s_j) \\
\beta_{j3}^{(i)} &= H_i^2(t) L_{0,2}(s_j) + \frac{\delta t}{2} U_{x,i}^n H_i^2(t) L_{0,2}(s_j) + \frac{\delta t}{2H_i(t)} U_i^n H_i^2(t) L'_{0,2}(s_j) + \frac{\delta t}{2H_i^2(t)} H_i^2(t) L''_{0,2}(s_j) + \frac{\delta t}{2H_i^4(t)} H_i^2(t) L_{0,2}^{(iv)}(s_j) \\
\beta_{j4}^{(i)} &= H_i^3(t) L_{0,3}(s_j) + \frac{\delta t}{2} U_{x,i}^n H_i^3(t) L_{0,3}(s_j) + \frac{\delta t}{2H_i(t)} U_i^n H_i^3(t) L'_{0,3}(s_j) + \frac{\delta t}{2H_i^2(t)} H_i^3(t) L''_{0,3}(s_j) + \frac{\delta t}{2H_i^4(t)} H_i^3(t) L_{0,3}^{(iv)}(s_j) \\
\beta_{j5}^{(i)} &= L_{1,0}(s_j) + \frac{\delta t}{2} U_{x,i}^n L_{1,0}(s_j) + \frac{\delta t}{2H_i(t)} U_i^n L'_{1,0}(s_j) + \frac{\delta t}{2H_i^2(t)} L''_{1,0}(s_j) + \frac{\delta t}{2H_i^4(t)} L_{1,0}^{(iv)}(s_j) \\
\beta_{j6}^{(i)} &= H_i(t) L_{1,1}(s_j) + \frac{\delta t}{2} U_{x,i}^n H_i(t) L_{1,1}(s_j) + \frac{\delta t}{2H_i(t)} U_i^n H_i(t) L'_{1,1}(s_j) + \frac{\delta t}{2H_i^2(t)} H_i(t) L''_{1,1}(s_j) + \frac{\delta t}{2H_i^4(t)} H_i(t) L_{1,1}^{(iv)}(s_j) \\
\beta_{j7}^{(i)} &= H_i^2(t) L_{1,2}(s_j) + \frac{\delta t}{2} U_{x,i}^n H_i^2(t) L_{1,2}(s_j) + \frac{\delta t}{2H_i(t)} U_i^n H_i^2(t) L'_{1,2}(s_j) + \frac{\delta t}{2H_i^2(t)} H_i^2(t) L''_{1,2}(s_j) + \frac{\delta t}{2H_i^4(t)} H_i^2(t) L_{1,2}^{(iv)}(s_j) \\
\beta_{j8}^{(i)} &= H_i^3(t) L_{1,3}(s_j) + \frac{\delta t}{2} U_{x,i}^n H_i^3(t) L_{1,3}(s_j) + \frac{\delta t}{2H_i(t)} U_i^n H_i^3(t) L'_{1,3}(s_j) + \frac{\delta t}{2H_i^2(t)} H_i^3(t) L''_{1,3}(s_j) + \frac{\delta t}{2H_i^4(t)} H_i^3(t) L_{1,3}^{(iv)}(s_j)
\end{aligned}
\tag{20}
$$

From the boundary conditions (28) and (29), one gets

$$
\begin{aligned}
U(x_1) &= \sigma \\
U_x(x_1) &= \beta \\
U(x_{N+1}) &= \omega \\
U_x(x_{N+1}) &= \zeta
\end{aligned}
\tag{21}
$$

which results in a consistent system of $4N + 4$ equations in $4N + 4$ unknowns.

5. Solution approach for the PDE system

The PDE system is solved using the rezoning approach which works best with the decoupled solution procedure [20]. The rezoning approach allow varying criteria of convergence for the mesh and physical equation since in practice the mesh does not require the same level of accuracy to compute as compared to the physical solution. The algorithm for the rezoning approach is as follows:

1. Solve the given physical PDE on the current mesh.
2. Use the PDE solution obtained to calculate the monitor function.
3. Find the new mesh by solving a MMPDE.
4. Adjust the current PDE solution to suite the new mesh by interpolation.
5. Solve the physical PDE on the new mesh for the solution in the next time.

http://dx.doi.org/10.5772/intechopen.71875

6. Solution adjustment by interpolation

Discretization of the time domain $[t_a, t_b]$ is done using the following finite sequence

$$\{t_a = t_0 < \ldots < t_n < \ldots < t_k = t_b\} \tag{22}$$

At each time $t = t_n = n \times dt$, consider a non-uniform spatial mesh $\{X_i^n\}_{i=1}^{N+1}$ given by

$$a = X_1^n < \ldots < X_{N+1}^n = b \tag{23}$$

where $X_i^n = X_i(t_n)$ with $H_i^n = X_{i+1}^n - X_i^n$ being a non-uniform spatial step for $i = 1, \ldots, N$. At the same time step $t = t_n$ one also considers the approximations to the exact solution $u(x, t)$ and its derivatives given by $\{U_i^n\}_{i=1}^{N+1}$ and $\left\{\left(U_i^{(l)}\right)^n\right\}_{i=1}^{N+1}$ respectively where $\left(U_i^{(l)}\right)^n$ represents the l^{th} derivative approximation with respect to the variable x at the time $t = t_n$ For $l = 1, 2, 3$. A new mesh $\left\{\tilde{X}_i^n\right\}_{i=1}^{N+1}$ is generated by (2) at each current time step t_n. The goal is to determine the new approximations $\left\{\tilde{U}_i^n\right\}_{i=1}^{N+1}$ and $\left\{\left(\tilde{U}_i^{(l)}\right)^n\right\}_{i=1}^{N+1}$ which are related to the new mesh $\left\{\tilde{X}_i^n\right\}_{i=1}^{N+1}$ in a similar manner the approximations $\{U_i^n\}_{i=1}^{N+1}$ and $\left\{\left(U_i^{(l)}\right)^n\right\}_{i=1}^{N+1}$ are related to the old mesh $\{X_i^n\}_{i=1}^{N+1}$ in each subinterval $[X_i, X_{i+1}]$. This process of updating the solution and its derivatives from the old mesh to the new mesh is achieved by interpolation. One considers the septic Hermite interpolating polynomial, a piecewise polynomial which allows the function values and its three consecutive derivatives to be satisfied in each subinterval $[X_i, X_{i+1}]$. The Hermite polynomial (14) is written in compact form as

$$\sum_{l=0}^{3} (h_l)^{(l)} U_i^{(l)} L_{0,l}(s) + \sum_{l=0}^{3} (h_l)^{(l)} U_{i+1}^{(l)} L_{1,l}(s) \tag{24}$$

where the $4(N + 1)$ unknowns are given by

$$U_i^{(i)} = \frac{\partial^l u}{\partial x^l}(X_i(t), t) U_{i+1}^{(l)} \approx \frac{\partial^l u}{\partial x^l}(X_{i+1}(t), t), \quad l = 0, 1, 2, 3.$$

Given the partition (23) and approximations $\left\{\left(U_i^{(l)}\right)^n\right\}$ for $l = 0, 1, 2, 3$, suppose interpolation of $U^{(l)}(x)$ is required at $x = \tilde{X}_i{}^n$ where $\tilde{X}_i{}^n \in \left[X_i^n, X_{i+1}^n\right]$ for $i = 1, \ldots, N$. Firstly, the local coordinate s of $\tilde{X}_i{}^n$ is defined as

$$s = \frac{\tilde{X}_i{}^n - X_i^n}{H_i^n} \tag{25}$$

$\tilde{U}^{(l)}\left(\tilde{X}_i{}^n\right)$ is then defined as

$$\tilde{U}^{(l)}\left(\tilde{X}_i{}^n\right) = \sum_{i=0}^{3} H_i^{l-p} U_i^{(l)} \frac{d^{(l)} L_{0,l}(s)}{ds^{(l)}} + \sum_{i=0}^{3} H_i^{l-p} U_{i+1}^{(l)} \frac{d^{(l)} L_{0,l}(s)}{ds^{(l)}} \tag{26}$$

for $l = 0, 1, 2, 3$ to give the interpolated values of $\tilde{U}$ and the first three consecutive derivatives on the new subinterval $\left[\tilde{X}_i^n, \tilde{X}_{i+1}^n\right]$. In order to compute the approximations of U at the next time step $t = t_{n+1}$ denoted by $\left\{U_i^n\right\}_{i=1}^{N+1}$, the values of the new mesh $\left\{\tilde{X}_i^n\right\}_{i=1}^{N+1}$ and the updated approximations $\left\{\tilde{U}_i^n\right\}_{i=1}^{N+1}$ are used in a septic Hermite collocation numerical scheme. The new approximations $\left\{U_i^{n+1}\right\}_{i=1}^{N+1}$ and the new mesh $\left\{\tilde{X}_i^{n+1}\right\}_{i=1}^{N+1}$ become the starting conditions for repeating the whole adaptive process.

7. Numerical results

Consider the KSe

$$\frac{\partial u}{\partial t} + u\frac{\partial u}{\partial x} + \frac{\partial^2 u}{\partial x^2} + \frac{\partial^4 u}{\partial x^4} = 0, \qquad t > 0 \tag{27}$$

in the domain $[-30, 30]$, $t > 0$ with boundary conditions

$$u(-30, t) = \sigma, \qquad u_x(-30, t) = \beta \tag{28}$$

$$u(30, t) = \omega, \qquad u_x(30, t) = \zeta \tag{29}$$

Where σ, β, ω and ζ are obtained from the exact solution

$$u(x, t) = c + \frac{15}{19}\sqrt{\frac{11}{19}}\left[-9\tanh^3(k(x - ct - x_0)) + 11\tanh(k(x - ct - x_0))\right] \tag{30}$$

With $c = 0.1, x_0 = -12$ and $k = \frac{1}{2}\sqrt{\frac{11}{19}}$.

Figures 1 and **2** show the behaviour of the numerical solution and the absolute error, respectively of the KSe equation on a stationary mesh using Hermite collocation method at $t = 4$ with $N = 100$ and $\delta t = 0.001$. In **Figure 1**, one observes that the numerical solution tracks the exact solution with the absolute error variation as shown in **Figure 2**.

Figure 3 shows the solution obtained by the collocation method on a stationary mesh for time $t = 0, 1, 2, 3, 4$. The movement of the solution is from left to right as time increases and the solution tracks the exact solution with no oscillations. One also observes that the concentration of mesh points is higher in the flatter regions of the solution profile in comparison to the concentration in the steeper region.

http://dx.doi.org/10.5772/intechopen.71875

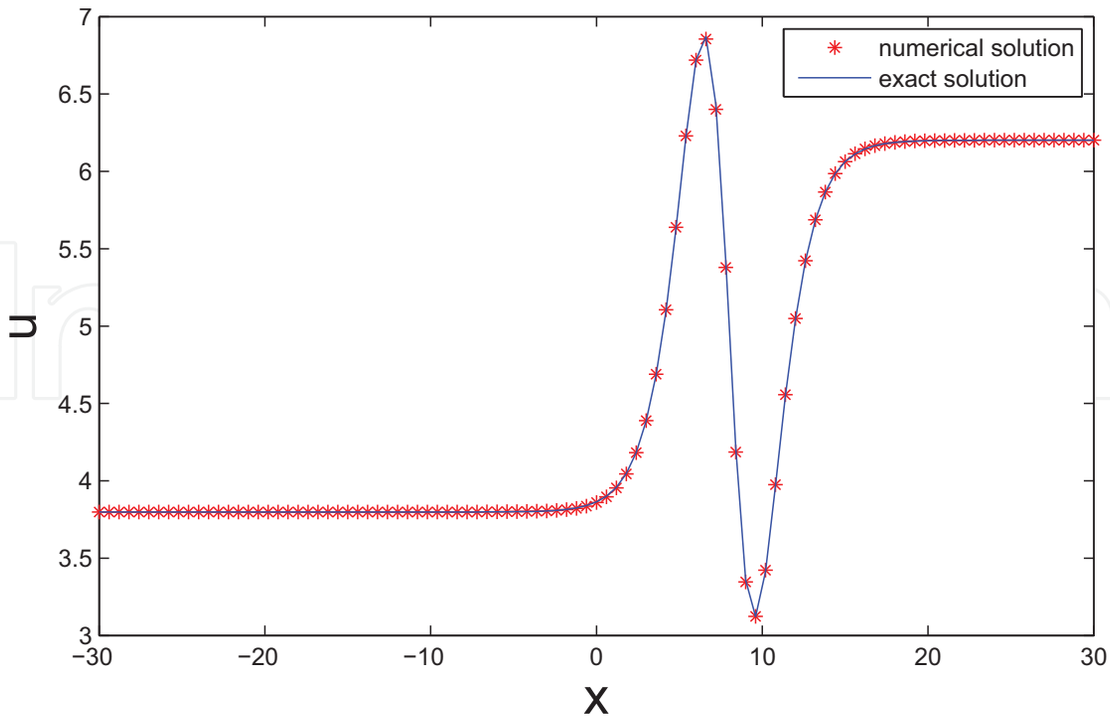

Figure 1. Hermite collocation method, uniform mesh, numerical solution behaviour of KSe at $t = 4$ with $N = 100$ and $\delta t = 0.001$.

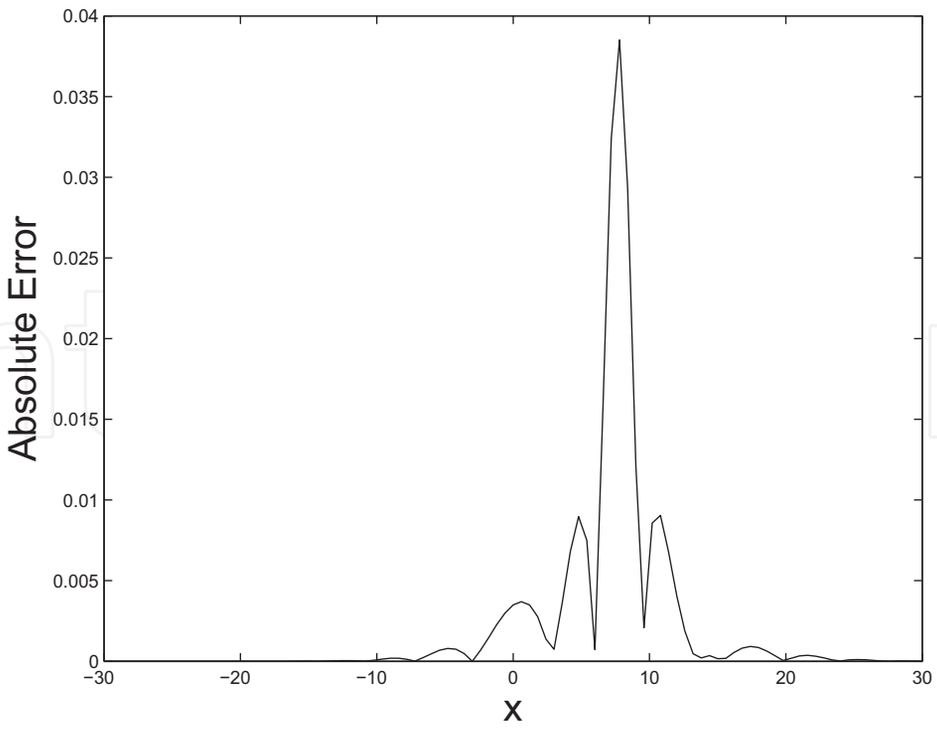

Figure 2. Hermite collocation method, uniform mesh, absolute error in numerical solution of KSe at $t = 4, N = 100$ and $\delta t = 0.001$.

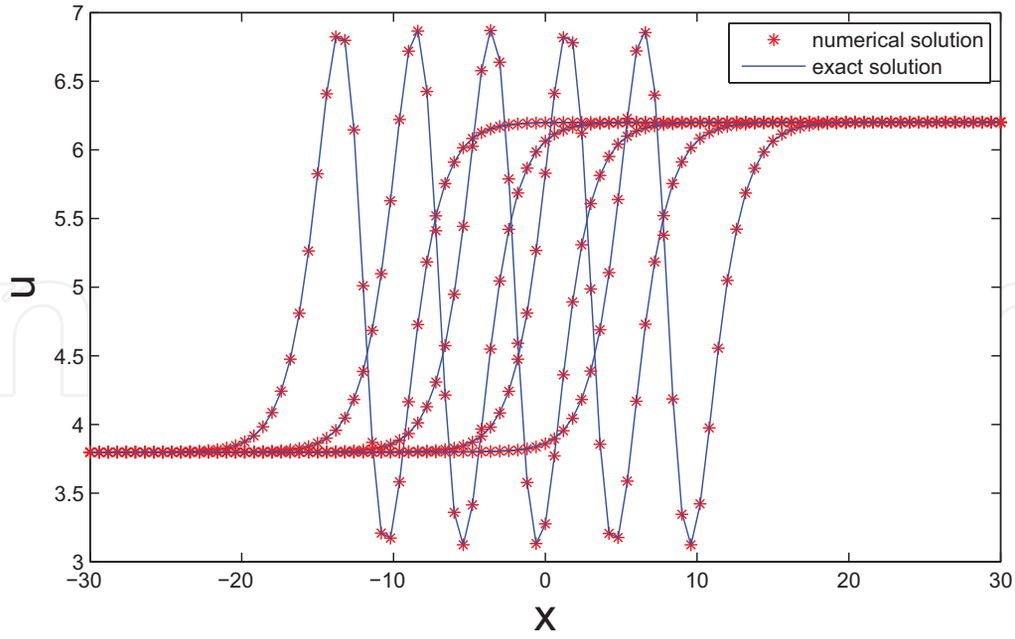

Figure 3. Hermite collocation method, stationary mesh, numerical solution behaviour of KSe problem with $N = 100$, $\delta t = 0.001$ up to final time $T = 4$.

Figures 4 and **5** show the numerical solution profile and the behaviour of the maximum absolute error, respectively at $t = 4$ with $N = 100, \delta t = 0.001$ and $\alpha = 8$ on an adaptive mesh. In **Figure 4**, one observes that the numerical solution is able to track the exact solution and the distribution of mesh points is almost equal along the solution profile which enables resolution of the solution with minimum errors.

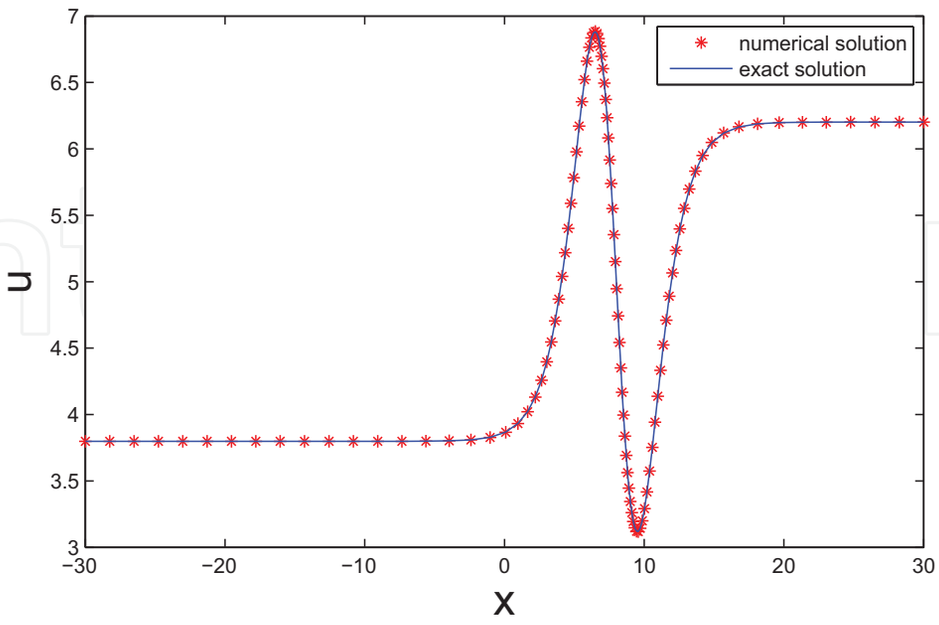

Figure 4. Hermite collocation method, non-uniform mesh, numerical solution behaviour of KSe problem at $t = 4$ with $N = 100, \delta t = 0.001, \tau = 2 \times 10^{-2}$ and $\alpha = 8$.

http://dx.doi.org/10.5772/intechopen.71875

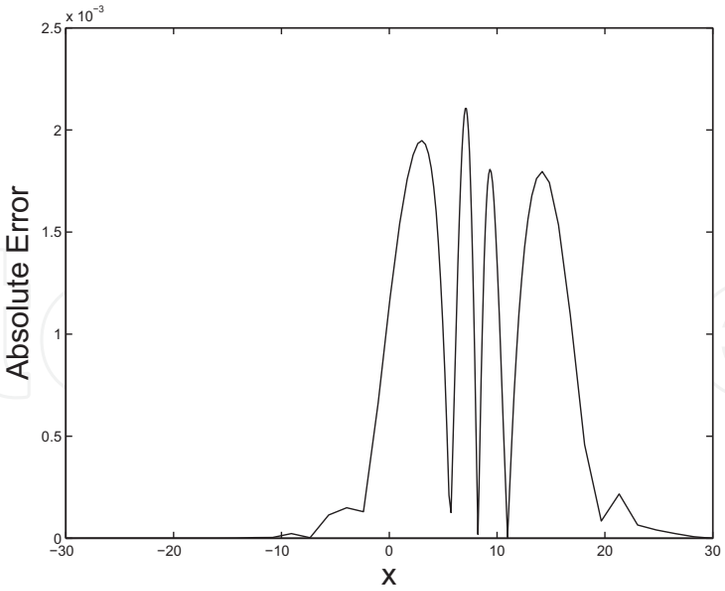

Figure 5. Hermite collocation method, non-uniform mesh, absolute error in numerical solution of KSe at $t = 100$, $\delta t = 0.001$, $\tau = 2 \times 10^{-2}$ and $\alpha = 8$.

Figure 6 shows the numerical solution profiles produced by the adaptive collocation method for time $t = 0, 1, 2, 3, 4$. One observes that the solution moves from left to right as time progresses. The mesh points at different times keep on tracking the solution profile and maintain an almost equal distribution along the profile up to final time $T = 4$. **Figure 7** shows the paths taken by the mesh points in tracking the solution profile. In **Table 1**, the infinity norm error for an adaptive collocation method is calculated and results are compared with the method in [13]. Results show improvements in the maximum point wise errors when an adaptive Hermite collocation method is used.

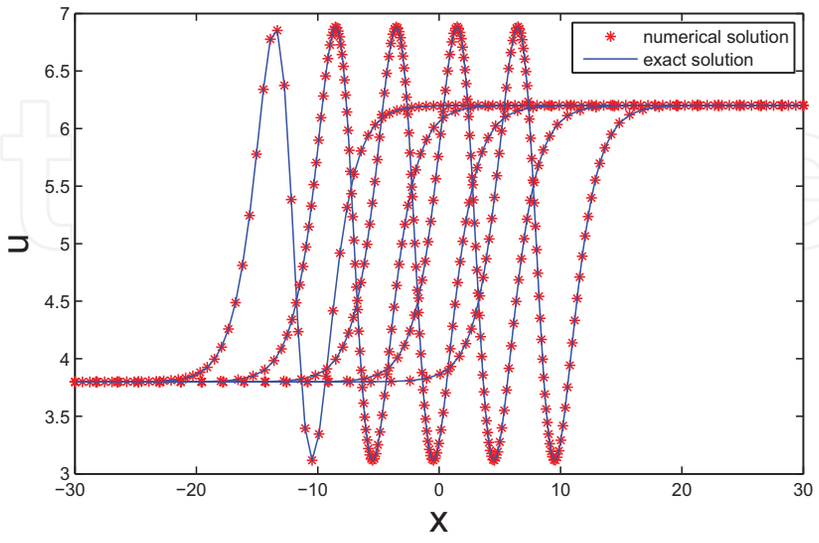

Figure 6. Hermite collocation method, adaptive mesh, numerical solution behaviour of KSe up to final time $T = 4$ for $N = 100$, $\delta t = 0.001$, $\tau = 2 \times 10^{-2}$ and $\alpha = 8$.

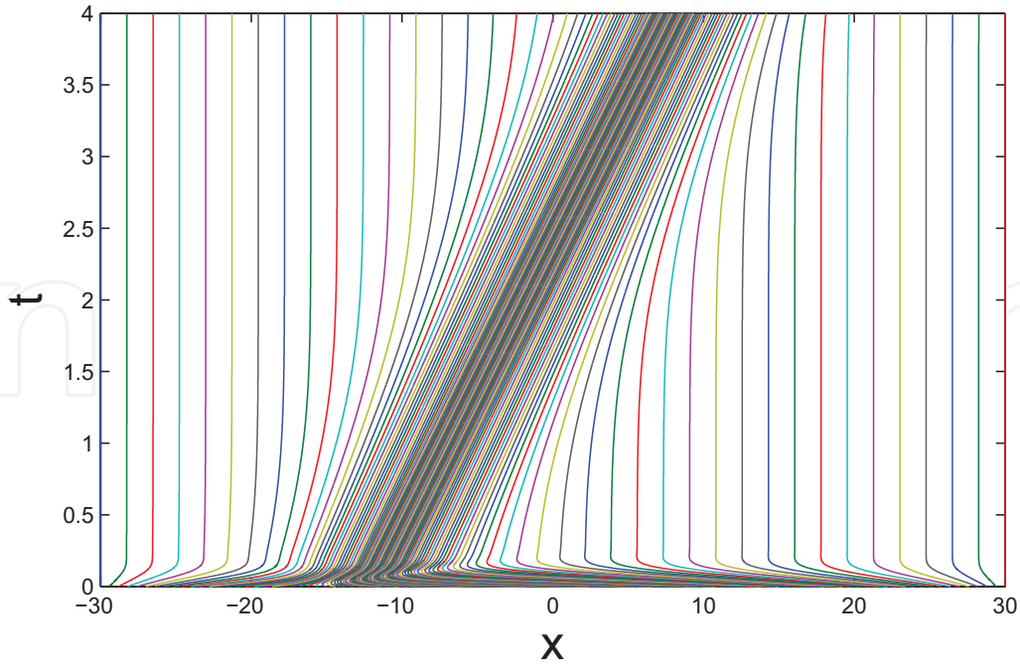

Figure 7. Hermite collocation method, mesh trajectories of KSe equation up to final time $T = 4$ with $N = 100$, $\delta t = 0.001$, $\tau = 2 \times 10^{-2}$ and $\alpha = 8$.

Time	Hermite collocation	Method in [19]
0.5	9.0×10^{-4}	1.03619×10^{-3}
1	1.4×10^{-3}	1.63762×10^{-3}
1.5	1.9×10^{-3}	2.07273×10^{-3}
2	1.7×10^{-3}	2.48375×10^{-3}
2.5	2.0×10^{-3}	2.79434×10^{-3}
3	2.1×10^{-3}	3.00439×10^{-3}
3.5	2.1×10^{-3}	3.16038×10^{-3}
4	2.1×10^{-3}	3.43704×10^{-3}

Table 1. Comparison of maximum pointwise errors in the numerical solution of the KSe on an adaptive mesh at different times with $\delta t = 0.001$ and $N = 100$.

8. Conclusions

The KSe is solved using an adaptive mesh method with discretization in the spatial domain done using seventh order Hermite basis functions. Numerical results show that Hermite collocation method on a non-uniform adaptive mesh is able to improve the accuracy of the numerical solution of the KSe. The method is able to keep track of the region of rapid solution variation in the KSe, which is one of the desired properties of an adaptive mesh method.

Author details

Denson Muzadziwa[1], Stephen T. Sikwila[2] and Stanford Shateyi[3]*

*Address all correspondence to: stanford.shateyi@univen.ac.za

1 University of Zimbabwe, Harare, Zimbabwe

2 Sol Plaatje University, Kimberley, South Africa

3 University of Venda, Thohoyandou, South Africa

References

[1] Sivashinsky GI. Nonlinear analysis of hydrodynamic instability in laminar flames-I-derivation of basic equations. Acta Astronautica. 1977;**4**:1177-1206

[2] Kuramoto Y. Diffusion-induced chaos in reaction systems. Supplement of the Progress of Theoretical Physics. 1978;**64**:346-367

[3] Kuramoto Y. Instability and turbulence of wavefronts in reaction-diffusion systems. Progress of Theoretical Physics. 1980;**63**:1885-1903

[4] Kuramoto Y, Tsuzuki T. Diffusion-induced chaos in reaction systems. Progress of Theoretical Physics. 1975;**54**:689-699

[5] Kuramoto Y, Tsuzuki T. Persistent propagation of concentration waves in dissipative media far from thermal equilibrium. Progress of Theoretical Physics. 1976;**55**:356-369

[6] Hooper AP, Grimshaw C. Nonlinear instability at the interface between two viscous fluids. Physics of Fluids. 1985;**28**:37-45

[7] Sivashinsky GI, Michelson D. On irregular wavy flow of a liquid film down a vertical plane. Progress in Theoretical Physics. 1980;**63**:2112-2114

[8] Khater AH, Temsah RS. Numerical solution of the generalised Kuramoto-Sivashinsky equation by Chebyshev spectral collocation method. Computers and Mathematics Applications. 2008;**56**:1465-1472

[9] Mittal RC, Arora G. Quintic b-spline collocation method for numerical solution of the Kuramoto-Sivashinsky equation. Communications in Nonlinear Science and Numerical Simulation. 2010;**15**(10):2798-2808

[10] Huilin L, Changfeng M. Lattice Boltzmann method for the generalised Kuramoto-Sivashinsky equation. Physica A: Statistical Mechanics and its Applications. 2009;**388**(8):1405-1412

[11] Haq S, Bibi N, Tirmizi SI, Usman M. Meshless method of lines for the numerical solution of the Kuramoto-Sivashinsky equation. Applied Mathematics and Computation. 2010; **217**(6):2404-2413

[12] Zavalani G. Fourier spectral collocation method for the numerical solving of the Kuramoto-Sivashinsky equation. American Journal of Numerical Analysis. 2014;**2**(3):90-97

[13] Zarebnia M, Parvaz R. Septic b-spline collocation method for numerical solution of the Kuramoto-Sivashinsky equation. Communications in Nonlinear Science and Numerical Simulation. 2013;**7**(3):354-358

[14] Hawken DF, Gottlieb JJ, Hansen JS. Review of some adaptive node movement techniques in finite element and finite difference solutions of PDEs. Journal of Computational Physics. 1991;**95**(2):254-302

[15] Huang W, Ren Y, Russell RD. Moving mesh methods based on moving mesh partial differential equations. Journal of Computational Physics. 1994;**113**:279-290

[16] Huang W, Ren Y, Russell RD. Moving mesh partial differential equations based on equi-distribution principle. SIAM Journal on Numerical Analysis. 1994;**31**(3):709-730

[17] De Boor C. Good approximation by splines with variable knots. ii. In: Conference on the Numerical Solution of Differential Equations. 1974;**363**:12-20

[18] Rubin SG, Graves RA. Cubic Spline Approximation for Problems in Fluid Mechanics. Washington DC: NASA; 1975. 93 p

[19] Russell RD, Williams JF, Xu X. MOVCOL4: A moving mesh code for fourth-order time-dependent partial differential equations. SIAM Journal on Scientific Computing. 2007;**29**(1): 197-220

[20] Weizhang H, Russell RD. Adaptive Moving Mesh Methods. New York: Springer; 2010. 432 p